



Magnetoresistivity of hydrogen-doped $Zr_2(3d)$ metallic glasses



M. Novak ^{*},¹, I. Kokanović

Department of Physics, Faculty of Science, University of Zagreb, Bijenička cesta 32, HR-10002 Zagreb, Croatia

ARTICLE INFO

Article history:

Received 19 March 2013

Received in revised form 17 May 2013

Available online 15 June 2013

Keywords:

Metallic glasses;
Magnetoresistivity;
Hydrogen doping;
Weak-localization;
Spin fluctuations

ABSTRACT

Magnetoresistivity of $(Zr_2(3d))_{1-x}H_x$ metallic glasses (where 3d stands for Fe and Co atoms) was investigated as a function of hydrogen doping (x) in the temperature range from 100 K down to 5 K. Obtained magnetoresistivity is always positive due to the strong spin–orbit interaction and well described in the terms of exchange-enhanced spin-splitting contributions to the usual weak-localization term. $(Zr_2Fe)_{1-x}H_x$ exhibits a significantly stronger magnetoresistivity than $(Zr_2Co)_{1-x}H_x$ for all measured temperatures and doping levels, which is attributed to the increase in the inelastic spin-scattering rate (τ_{in}^{-1}) and the Stoner factor $(1-I)^{-1}$. The magnetoresistivity of $(Zr_2(3d))_{1-x}H_x$ exhibits a simple B^2 behavior at higher temperatures, providing the information on τ_{in}^{-1} , and a more complex behavior at low temperatures, which gives the information on the spin–orbit scattering rate (τ_{so}^{-1}). It was found that the increase in the doping level reduces τ_{so}^{-1} , indicating hybridization of hydrogen s-electrons with Zr d-electrons and thus reducing the spin–orbit interaction.

© 2013 Elsevier B.V. All rights reserved.

1. Introduction

The complex nature of electron transport in Zr-based metallic glasses at low temperatures is still controversial [1–6]. Metallic glasses based on Zr are especially interesting because they exhibit a low temperature interplay between the superconductivity and magnetism, changing the configuration from superconducting to highly enhanced paramagnetic with the substitution of Co atoms with Fe atoms [1,7,8]. For example Zr_2Fe metallic glass has higher electronic density of states at the Fermi level than Zr_2Co , but it is not superconducting. It has been shown that dT_c/dy (y being the Zr concentration) actually diverges close to $y = 0.71$; T_c being 0.6 K for $y = 0.72$ and less than 0.06 K for $y = 0.71$ [7]. The collapse of T_c has been explained by the occurrence of the spin fluctuations and formation of the localized magnetic moments at the Fe atomic sites. Thus, $(Zr_2Fe)_{1-x}H_x$ metallic glasses represent a good matrix for examining the spin fluctuations and the formation of the magnetic moments in a highly disordered system, since the level of spin fluctuations and the formation of the magnetic moments can be tuned by the level of hydrogen doping (x) [9].

A highly disordered structure of the metallic glasses such as Zr_23d makes the motion of the charge carriers not ballistic, but diffusive, which entails quantum corrections to the Boltzmann transport equation [10]. In the metallic glasses the phase conserving elastic scattering time (τ_e) at low temperatures is usually several orders of magnitude

smaller than the dephasing scattering time (e.g. the inelastic scattering time (τ_{in}) or the spin–orbit scattering time (τ_{so})), hence the weak-localization effects (WL) arising from the quantum interference of the electron wave functions have a significant effect on the electrical resistivity ($\rho(T)$) and magnetoresistivity (MR). Although the WL theory quantitatively describes the MR of superconducting transition-metal amorphous alloys well, significant deviations of both magnitude and temperature dependence occur in the non-superconducting systems. Trudeau and Cochrane have shown that the size and form of the MR for paramagnetic Zr–Fe alloys vary rapidly as a result of increasing Stoner factor [11]. The MR at some temperature (T) in the case of the WL interaction with the spin–orbit scattering and the Zeeman splitting is given by [10,12]:

$$\begin{aligned} \Delta\rho/\rho &= [\rho(B) - \rho]/\rho \\ &= -\rho A \left[\sqrt{h} F\left(\frac{1+t}{h}\right) + \frac{1}{2} \sqrt{\frac{h}{1-\gamma}} \left[F\left(\frac{t_+}{h}\right) - F\left(\frac{t_-}{h}\right) \right] \right] - \\ &\quad - \frac{1}{\sqrt{1-\gamma}} (\sqrt{t_-} - \sqrt{t_+}) + \sqrt{t_-} - \sqrt{t_+ + 1}, \end{aligned} \quad (1)$$

where $A \sim e^2 (D_e \tau_{so})^{-1/2} / 2\pi^2 \hbar$, $h = eBD_e \tau_{so} / \hbar$, $t = \tau_{so} / 4\tau_{in}$, $t_{\pm} = t + (1 \pm \sqrt{1-\gamma}) / 2$ and $\gamma = (g^* \mu_B B \tau_{so} / 2(1-I)\hbar)^2$ a factor which arises from the Zeeman splitting effect, D_e is the electron diffusion constant, the reduced Planck constant, μ_B the Bohr magneton, $(1-I)^{-1}$ the Stoner factor and g^* is an effective g -factor. The inelastic scattering process characterized by τ_{in} always gives a negative contribution to the MR, whereas the spin–orbit scattering and the Zeeman splitting give a positive contribution to the MR. If $\tau_{so} \ll (\tau_{in}, \tau_B)$, where $\tau_B = \hbar / 4BeD_e$, i.e.

^{*} Corresponding author.

E-mail addresses: mnovak@phy.hr (M. Novak), kivan@phy.hr (I. Kokanović).

¹ Present address: Institute of Scientific and Industrial Research, Osaka University, Ibaraki, Osaka 567-0047, Japan.

the strong spin–orbit scattering case, Eq. (1) gives a positive MR with $\Delta\rho \propto B^2$ for small magnetic fields ($\tau_{in} < \tau_B$) and $\Delta\rho \propto \sqrt{B}$ for large magnetic fields ($\tau_B < \tau_{in}$) [13]. The temperature dependence of $\Delta\rho(B, T)$ is dominantly governed by $\tau_{in} \propto T^{-p}$, where $p = 2$ at low T , since τ_{so} is usually regarded as T independent [14,15]. The function $F(x)$ in Eq. (1) is defined as:

$$F(x) = \sum_{n=0}^{\infty} \left[2(\sqrt{n+1+x} - \sqrt{n+x}) - \frac{1}{\sqrt{n+x+1/2}} \right], \quad (2)$$

with the limiting forms $F(x) = 0.605$ for $x \ll 1$ and $F(x) = x^{-3/2}/48$ for $x \gg 1$.

If the MR is measured at the T close to the superconducting-transition temperature (T_c) effects of the superconducting fluctuations have to be taken into account. The Maki–Thompson contribution to the MR due to the superconducting fluctuation is:

$$\Delta\rho(B, T)/\rho = \rho A \sqrt{\hbar} \beta(B, T) F(t/\hbar), \quad (3)$$

where $\beta(T, B)$ represents the Maki–Thompson interaction [16].

This paper presents a systematic study of the MR of $(Zr_23d)_{1-x}H_x$ ($3d = Fe$ and Co) metallic glasses upon hydrogen doping. The hydrogen is used as a light atomic probe for studying the quantum interference effects on the magnetotransport by changing the local scattering environment through the hybridization of hydrogen with the host matrix. Doping the samples with hydrogen increases disorder. Thus, by changing the hydrogen concentration the effects of electron localization, spin fluctuations and electron–electron interaction have been continuously varied and their interplay studied in a controlled way. Due to a small size hydrogen can be effectively and homogeneously distributed throughout the sample. The MR was measured in the temperature range from 5 K up to 100 K in magnetic field up to 7 T. It was found that the MR is always positive in the measured T and B ranges. Although Zr_2Fe and Zr_2Co have a similar room temperature resistivity $\approx 180 \mu\Omega\text{cm}$, their $\rho(T)$ and $\Delta\rho/\rho$ show significantly different behavior. At low T the transport properties of $(Zr_2Fe)_{1-x}H_x$ show effects of the spin fluctuations, whereas $(Zr_2Co)_{1-x}H_x$ exhibits superconductivity. The MR decreases when Fe atoms are replaced with Co atoms, but for the both systems the MR increases with increasing x . Increasing x also reduces the effective electron-diffusion constant D_e and the spin-orbit scattering rate τ_{so}^{-1} . The high- T MR follows $\Delta\rho/\rho \propto (B/T)^2$, which reveals T^{-2} dependence of the $\tau_{in}(T)$, whereas the low- T MR reveals a more complex behavior providing information on τ_{so}^{-1} .

2. Experimental method

Ribbons of Zr_2Fe and Zr_2Co metallic glasses were prepared by rapid solidification of the melt on a single-roll spinning copper wheel in an argon atmosphere. The samples, 1–2 cm long, 1.5 mm wide and 25 μm thick were then cut from the same ribbon. The hydrogenation was carried out electrolytically and the concentrations were determined volumetrically using a McLeod manometer [9,17]. The as-quenched and hydrogenated samples were examined by X-ray diffraction, using $\text{Cu-K}\alpha$ ($\lambda = 0.15418 \text{ nm}$) radiation to verify they were amorphous.

The low- T MR was measured by the four-probe DC method in the temperature range from 5 K up to 100 K using a VTI equipped He-cryostat system. During the measurement the sample current and the magnetic field were orientated in the transversal configuration. The point size current and voltage contacts are made by the spot-welding method.

3. Results and discussion

Fig. 1 presents the MR of $(Zr_2Fe)_{1-x}H_x$ at 5 K for the four different levels of doping: $x = 0.0, 0.07, 0.09$ and 0.19 . In addition, the MR of

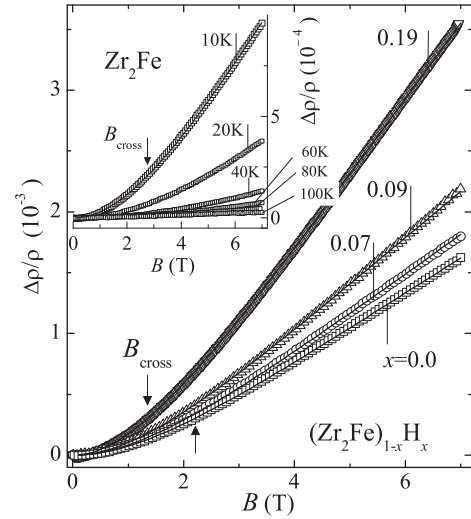


Fig. 1. (Main panel) The MR of $(Zr_2Fe)_{1-x}H_x$ at $T = 5 \text{ K}$ for $x = 0.0, 0.07, 0.09$ and 0.19 . The MR shows B^2 dependence for small fields and fairly linear dependence for larger fields ($B > 2T$) and increases by increasing x . Solid lines represent the best fit of Eq. (1) to the experimental data. The vertical arrow marks B_{cross} , a maximal B for which the MR is still quadratic. (Inset) The MR of Zr_2Fe versus B at several different temperatures as indicated.

the undoped Zr_2Fe sample at several higher temperatures is shown in the inset to Fig. 1. Solid lines in Fig. 1 are the best fit of Eq. (1) to the experimental data with the fit values given in Table 1.

The MR of $(Zr_2Fe)_{1-x}H_x$ is positive indicating the strong spin–orbit interaction, increases with the hydrogen doping and decreases with increasing T .

At the low T , (5 K and 10 K) $\Delta\rho/\rho$ shows B^2 dependence only for small magnetic fields. The maximal magnetic field (B_{cross}) for which B^2 law is still valid at 5 K is around 2.1 T for $x = 0$ and decreases with increasing x down to 1.6 T for $x = 0.19$. With increasing temperature B_{cross} is shifted to higher values and for $T \geq 40 \text{ K}$ the B^2 dependence is seen for the whole measured B range (see Fig. 2). The B^2 dependence is valid if $\tau_{in} < \tau_B$, giving a crude estimation of $\tau_{in} \sim 3 \cdot 10^{-12} \text{ s}$ at $T = 5 \text{ K}$, which is in a good agreement with the values in Table 1. The observed decrease in the slope of the MR with increasing T in Fig. 2 for Zr_2Fe is attributed to the decrease of τ_{in} .

To get a better insight in the underlying physics of the magneto-transport we have also analyzed the MR of $(Zr_2Co)_{1-x}H_x$ metallic glass, where Fe atoms are replaced with the less magnetic Co atoms. The resistivity measurements on $(Zr_2Fe)_{1-x}H_x$ have shown that $\rho(T)$ is dominated by the WL mechanism with the strong spin–orbit scattering at the high T , and the electron–electron interaction and spin-fluctuation at the low T eNovak2012. The substitution of Fe with Co atoms has revealed a significant impact on $\rho(T)$. The $(Zr_2Co)_{1-x}H_x$ system becomes superconducting and shows no effects of the spin-fluctuations at the low T , i.e. $\rho(T)$ is only governed by the WL effects with the strong spin–

Table 1

Electron-diffusion constant D_e , spin–orbit scattering time τ_{so} , inelastic scattering time τ_{in} and the Stoner factor $(1 - I)^{-1}$ for $(Zr_2Fe)_{1-x}H_x$ (at 5 K) and $(Zr_2Co)_{1-x}H_x$ (at 10 K).

	x	D_e $10^{-5} \text{ m}^2 \text{ s}^{-1}$	τ_{so} 10^{-13} s	τ_{in} 10^{-12} s	$(1 - I)^{-1}$
Zr_2Fe	0.0	3.8	2.1	4.4	3.29
	0.07	3.7	2.6	3.8	3.23
	0.09	3.7	2.6	3.3	3.4
	0.19	3.5	3.3	2.3	3.5
Zr_2Co	0	6.4	1.2	2.2	
	0.07	6.2	1.5	3.8	
	0.09	6.1	1.8	4.2	
	0.15	5.9	2.3	4.5	

Download English Version:

<https://daneshyari.com/en/article/7903678>

Download Persian Version:

<https://daneshyari.com/article/7903678>

[Daneshyari.com](https://daneshyari.com)